Journal of Nuclear Materials 398 (2010) 139–145

Contents lists available at ScienceDirect

Journal of Nuclear Materials

journal homepage: www.elsevier.com/locate/jnucmat

# Corrosion characteristics of materials in Pb–Bi under transient temperature conditions

Abu Khalid Rivai [a,*], Minoru Takahashi [b,1]

[a] Department of Nuclear Engineering, Graduate School of Science and Engineering, Tokyo Institute of Technology, N1-18, 2-12-1, O-okayama, Meguro-ku, Tokyo 152-8550, Japan
[b] Research Laboratory for Nuclear Reactors, Tokyo Institute of Technology, N1-18, 2-12-1, O-okayama, Meguro-ku, Tokyo 152-8550, Japan

## ABSTRACT

Corrosion characteristics of materials in Pb–Bi under transient temperature conditions in the range 550–800 °C have been investigated. Two cases of transient temperature conditions were carried out. For the case-1, the specimens were immersed in Pb–Bi at 550 °C for 12 h and then the temperature was increased up to 800 °C and kept there for 12 h. For the case-2, the specimens were immersed in Pb–Bi at 550 °C for around 500 h and then the temperature was increased up to 800 °C and kept there for 15 h. The tested materials were surface coated steels of Al-SUS304-sputtering-coated HCM12A and SUS316, high chromium steels of HCM12A, Recloy10 and SUS430, a refractory metal of molybdenum, and ceramics of SiC and $Ti_3SiC_2$. The results showed that there was no trace of any corrosion attack mechanisms of Pb–Bi into the Al-SUS304-sputtering-coated steels, the refractory metal, and the ceramics found, for all transient temperature conditions cases. On the other hand, corrosion attack mechanism of Pb–Bi was found for high chromium steels specimens in all cases.

## 1. Introduction

Heavy liquid metal lead alloy is one of the most attractive candidate materials for a coolant and a spallation target for future nuclear reactor systems, Lead alloy-cooled Fast Reactors – LFRs and Accelerator Driven System – ADS, because its favorable in chemical, physical, thermodynamics, and neutron properties [1–3]. However, the critical issue of compatibility of materials in the lead alloy environment, especially at high temperature, has to be solved.

Several types of corrosion-resistant materials have been expected for lead alloys nuclear reactor systems, i.e. surface-treated steels, high chromium steels, refractory metals and ceramics [1–15]. However, for practical application the materials have to have high corrosion resistance from corrosion attack of lead alloy not only under normal condition but also in the temporary anomalous conditions. The anomalous conditions followed by transient temperature will directly influence to the strength of the materials in the reactor. In the lead alloy environment increasing the temperature will increase the solubility of metals into the lead alloy which means increasing the dissolution attack of the lead alloy to the materials. Therefore, high corrosion-resistant materials must be employed to handle corrosion attack from the lead alloy not only under normal condition but also in the temporary anomalous condition especially for the fuel cladding. Related to the temporary anomalous conditions in the reactor, it was reported that the cladding temperature of LFRs suddenly rose up to near 800 °C for several minutes until hours when accidents occurred [16–18]. The maximum cladding temperature reached 792 °C due to ULOHS (Unprotected Loss of Heat Sink)/ULOF (Unprotected Loss of Flow) event [17]. The transient temperature occurred for about 15–17 h in the reactor due to an instantaneous total loss of secondary flow and primary coolant pump trip without any activity could be done to scram the core [18].

Several investigations related to the corrosion behavior of materials under transient temperature conditions of lead alloy were reported by some researchers. Corrosion of ODS steel after tested in Pb–Bi at temperatures changing from 550 °C to 650 °C and back every 800 h for 4800 h was observed [19]. The damage and the increasing of corrosion rate of austenitic steel AISI 316L and the ferritic-martensitic steel T91 after tested in Pb–Bi under transient temperature of 550–650 °C occurred [20]. However, up to now the data of corrosion investigation for various types of materials in lead alloy under transient temperature with various conditions are still limited. Moreover, the investigations of corrosion characteristics of materials under transient temperature at severe conditions which are related to the worst accidents of reactors are more limited. Therefore, the purpose of this present study is to investigate the corrosion characteristics of candidate materials for a lead alloy nuclear system in the liquid Pb–Bi under transient

---

[*] Corresponding author. Present address: Nuclear Transmutation Technology Group, J-PARC, Japan Atomic Energy Agency, Tokai-mura, Naka-gun, Ibaraki-ken 319-1195, Japan. Tel.: +81 29 282 6026; fax: +81 29 282 5671.

*E-mail addresses:* rivai.abukhalid@jaea.go.jp (A.K. Rivai), mtakahas@nr.titech.ac.jp (M. Takahashi).

[1] Tel./fax: +81 3 5734 2957.

0022-3115/$ - see front matter © 2009 Elsevier B.V. All rights reserved.
doi:10.1016/j.jnucmat.2009.10.024

temperature conditions. The materials that were investigated were Al-SUS304-sputtering coated steels using unbalanced magnetron sputtering (UBMS) technique, a refractory metal and ceramics. UBMS technique as the surface treatment steels method to protect the steels' surface from corrosion attack has been widely used because of the benefits of deposit adherent, fully dense films for pure metals and alloys [23–26]. It was reported that the UBMS technique could effectively protect the surface of steel from corrosion attack of Pb–Bi at 700 °C [4]. However, corrosion behavior of the sputtering layer produced by using UBMS technique to protect the steel from corrosion attack of Pb–Bi under transient temperature conditions is very limited. For comparison analysis, the results of high chromium steels as the conventional steels without coating after tested in Pb–Bi with the same time and conditions with alloy-sputtering coated steels are presented.

## 2. Experimental apparatus and procedure

### 2.1. Experimental apparatus

The corrosion tests were carried out in a pot-type liquid metal test apparatus as shown in Fig. 1. The detail of corrosion test apparatus was already described in Ref. [4]. The apparatus consists of a steam generator, a moisture dew-point sensor, a heater section, an oxygen sensor, a test pot and a gas exhaust system. An alumina crucible was used as the test pot for molten Pb–Bi. It contains an oxygen sensor, a molybdenum wire to detect the output signal of the sensor, a ceramics nozzle for gas injection and a thermocouple for Pb–Bi temperature measurement. The crucibles are 180 mm in length, 60 mm in outer diameter and 5 mm in thickness. The injection of mixture gas of Ar–Ar + 3%$H_2$-steam flows through a stainless steel tube and enters the test pot from the ceramics nozzle. The oxygen concentration controlling sensor was made of a sintered magnesia-stabilized zirconia electrolyte, i.e. MSZ. As an internal reference, oxygen-saturated bismuth ($Bi/Bi_2O_3$) fluid was used. The sensor output signal was detected by two molybdenum (Mo) wires, one inserted into the internal reference fluid in the cell of oxygen sensor, and the other into the Pb–Bi in the crucible. The electromotive force (EMF) signals were measured using an electrometer.

The experimental conditions are shown in Table 1. The specimens were immersed in Pb–Bi at 550 °C for 12 h and then the temperature was increased up to 800 °C and kept there for 12 h for case-1 as shown in Fig. 2. In the transient condition case-2, the specimens were immersed in Pb–Bi at 550 °C for around 500 h and then the temperature was increased up to 800 °C and kept there for 15 h as shown in Fig. 3.

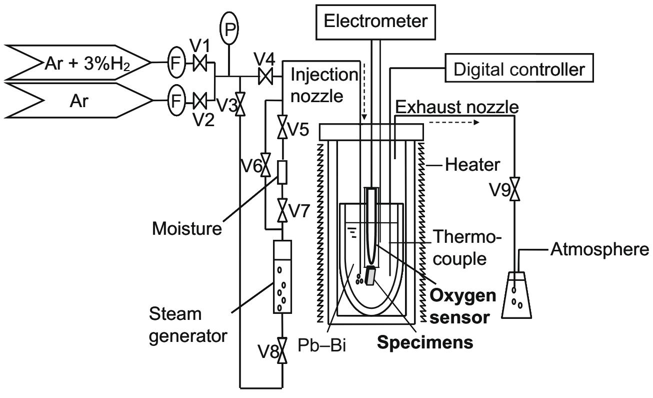

**Fig. 1.** Schematic of corrosion test apparatus.

### 2.2. Materials

Materials which were tested in this study were surface-treated steels, i.e. Al-SUS304-sputtering-coated steels, high chromium steels, a refractory metal and ceramics. Chemical compositions of these materials can be seen in Table 2.

The surface coated-steel specimens were Al-SUS304-sputtering coated HCM12A and SUS316 which were coated by Physical Vapor Deposition (PVD) technique using the UBMS (Unbalanced Magnetron Sputtering) method. The UBMS method which was applied in this study was already described in Ref. [4]. The UBMS technique was applied to HCM12A and SUS316 steels in two different times and conditions. Then, the Al-SUS304-sputtering coated HCM12A was tested under transient temperature case-1 and the Al-SUS304-sputtering coated SUS316 was tested under transient temperature case-2. The shapes of Al-SUS304-sputtering coated HCM12A and SUS316 were rectangular with 15 × 15 × 2 mm and 10 × 9.8 × 2 mm in sizes, respectively. Ar gas was used in this method to bombard the atoms of target materials where the sputtering target in this experiment was Al and SUS304. The use of the UBM sputtering technique has two advantages: the capability of uniform thickness of coating layer and fraction-controlled targets coating, and the formation of a strong bonding, related to adherent and full density, between the surface coating layer and the base metal [23–26].

For high chromium steels type, HCM12A, Recloy10, and SUS430 were tested. The HCM12A was tested under transient temperature case-1, and the Recloy10 and the SUS430 were tested under transient temperature case-2. The shapes of HCM12A, Recloy10 and SUS430 were rectangular with 15.3 × 4.8 × 2 mm, 10 × 5 × 1.6 mm and 12.5 × 5.2 × 1.9 mm in sizes, respectively. HCM12A which contains 12% Cr has been used for high-temperature components in power plants. Recloy10 which contains 18% Cr has been used in recuperators and heatproof protection tubes. SUS430 which contains 16% Cr has been used as structural materials for chemical plant. According to previous publications HCM12A, Recloy10 and SUS430 steels exhibited good performance to Pb–Bi at 550 °C [6,7].

The tested refractory metal was molybdenum. The molybdenum was tested for both cases of transient temperature conditions. The purity of the molybdenum specimen in this experiment was 99.95%. This material was supplied by the Nilaco Company. The shapes of molybdenum for transient temperature case-1 and case-2 were rectangular with 10.5 × 4.5 × 2 mm and 7.6 × 5.6 × 2 mm in sizes, respectively. According to the previous report, molybdenum exhibits high corrosion resistance to Pb–Bi at 700 °C [4].

For the ceramic materials, silicon carbide (SiC) and titanium silicon carbide ($Ti_3SiC_2$) were tested. The compositions of the SiC were 98SiC–0.2$SiO_2$–0.1Si–1.2C with 3.1 g/cm$^3$ in density. It was supplied by the Nilaco Company as well. The $Ti_3SiC_2$ is one of the new types of solids with 4.5 g/cm$^3$ in density. The Young's modulus is ∼325 GPa, and is readily machinable [21,22]. This specimen was supplied by the 3-ONE-2 LLC. The SiC and $Ti_3SiC_2$ for transient temperature case-1 and case-2 were rectangular with 15.2 × 4.5 × 2.3 mm and 15.2 × 6.3 × 2.3 mm in sizes for SiC, respectively, and 10.2 × 10 × 2 mm and 15 × 5.7 × 2.4 mm in sizes for $Ti_3SiC_2$, respectively. According to the previous report SiC and $Ti_3SiC_2$ exhibit high corrosion resistance to Pb–Bi at 700 °C [4].

### 2.3. Experimental procedure

The concentrations of oxygen were $10^{-6}$ (550 °C)–$2 \times 10^{-5}$ (800 °C) for the transient temperature case-1, and $10^{-6}$ wt% (550–800 °C) for the the transient temperature case-2. The Gromov's

**Table 1**
Experimental conditions.

| Parameter | I | II |
|---|---|---|
| Injection gas | Ar and Ar + 3%$H_2$ | Ar and Ar + 3%$H_2$ |
| Temperature of Pb–Bi (°C) | 550–800 | 550–800 |
| Oxy. concent. (wt%) | $10^{-6}$ (550 °C)–2 × $10^{-5}$ (800 °C) | $10^{-6}$ wt% (550–800 °C) |
| Specimens | Al-SUS304-sputtering-coated HCM12A; HCM12A; Mo; SiC; $Ti_3SiC_2$ | Al-SUS304-sputtering-coated SUS316; SUS430; Recloy10; Mo; SiC; $Ti_3SiC_2$ |
| Immersion time (h) | ~12 (at 550 °C) and ~12 (at 800 °C) | ~500 (at 550 °C) and ~15 (at 800 °C) |

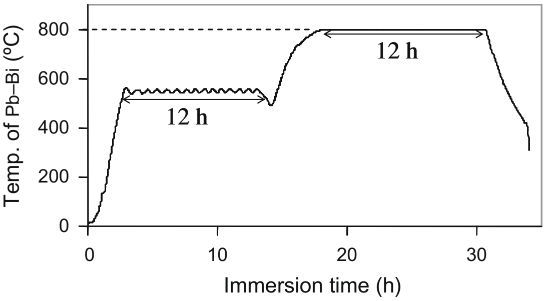

**Fig. 2.** Temperature profile of Pb–Bi under transient case-1.

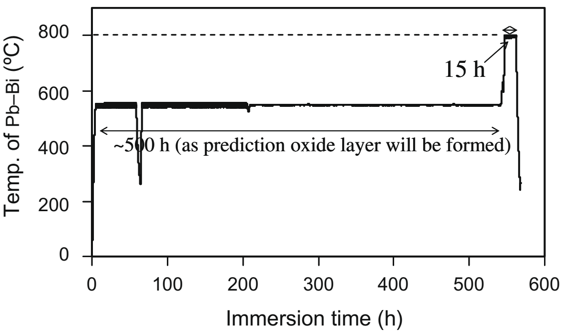

**Fig. 3.** Temperature profile of Pb–Bi under transient case-2.

oxygen solubility equation [1] was used to estimate the oxygen concentrations in Pb–Bi.

The corrosion characteristics of the tested materials were analyzed by the Scanning Electron Microscope (SEM)-Energy Dispersive X-ray Microanalysis (EDX). For analyzing purpose, the specimens were cut in the middle, solidified by resin and polished with a mechanical grinder using polycrystalline diamond grains.

## 3. Results

### 3.1. Transient temperature condition case-1

The aim of corrosion characteristics investigation of materials in Pb–Bi under the transient temperature condition case-1 is to predict the corrosion resistance of materials if temporary transient temperature occurs in the reactor in the early time of operation. In this case, there is no formation of oxide layer on the surface of the steels because of short time exposure to Pb–Bi. Therefore, the resistance of steels without the protection of a protective oxide layer could be observed. The results of testing under transient temperature condition case-1 are as follows.

Fig. 4 shows the SEM-EDX micrograph analysis of the cross section of HCM12A after immersion in Pb–Bi under transient temperature case-1. The results showed dissolution of constituent metals of iron and chromium atoms from the HCM12A matrix into Pb–Bi and penetration of Pb–Bi into the surface of HCM12A. The figure reveals that Pb atoms penetrated slightly deeper than Bi. This phenomenon has also been reported by other researchers [14,15]. Moreover, damage to the surface of HCM12A of 5–10 μm in depth was found. Fig. 4 also shows that there was no protective oxide layer formed which is similar to the prediction because of short time immersion in Pb–Bi. Therefore, there was no barrier layer to protect the surface of HCM12A from corrosion attack of Pb–Bi.

The specimen of Al-SUS304-sputtering coated HCM12A was tested in the same time and same conditions as HCM12A steel without coating. Fig. 5 shows the SEM-EDX micrograph analysis of the cross section of Al-SUS304-sputtering-coated HCM12A after immersion in Pb–Bi under transient temperature case-1. The figure shows that the coating layer remains intact on the base surface of the HCM12A. The results showed that there was no indication of dissolution of constituent metals from the matrix into Pb–Bi except for indication of small peak of nickel in the boundary between coating layer and adhered Pb–Bi. Moreover, no penetration of Pb–Bi into the matrix of material was observed.

The result of the molybdenum after immersion in Pb–Bi under transient temperature case-1 is shown in Fig. 6. The figure shows that no penetration of Pb–Bi into the matrix of material and no dissolution of molybdenum atoms from specimen into Pb–Bi. Moreover, no crack on the surface of the specimens after immersion in Pb–Bi under transient temperature up to 800 °C was observed. The results showed that the molybdenum exhibited high corrosion resistance to Pb–Bi under transient temperature case-1.

The results of ceramics are shown in Figs. 7 and 8. Fig. 7 shows the SEM-EDX micrograph analysis of the cross section of SiC after immersion in Pb–Bi under transient temperature case-1. The figure shows that no penetration of Pb–Bi into the matrix of material and no dissolution of constituent metal from specimen into Pb–Bi. Fig. 8 shows the EDX micrograph analysis of the cross section of

**Table 2**
Chemical compositions of the specimens (unit: wt%)

| Element/material | Fe | Cr | Mo | W | Si | Others |
|---|---|---|---|---|---|---|
| HCM12A | Balance | 12 | 0.3 | 1.9 | 0.3 | 0.9 Cu |
| SUS430 | Balance | 16.1 | – | – | 0.63 | 0.2 Mn |
| Recloy10 | Balance | 17.7 | – | | 1 | 0.9 Al |
| Sputtering-treated steels | Targets: Al-SUS304 (consisted of mainly Fe, 18–20 Cr and 8 Ni) | | | | | |
| Mo | 99.95 purity | | | | | |
| SiC | 98 SiC–0.2 $SiO_2$–0.1 Si–1.2 C | | | | | |

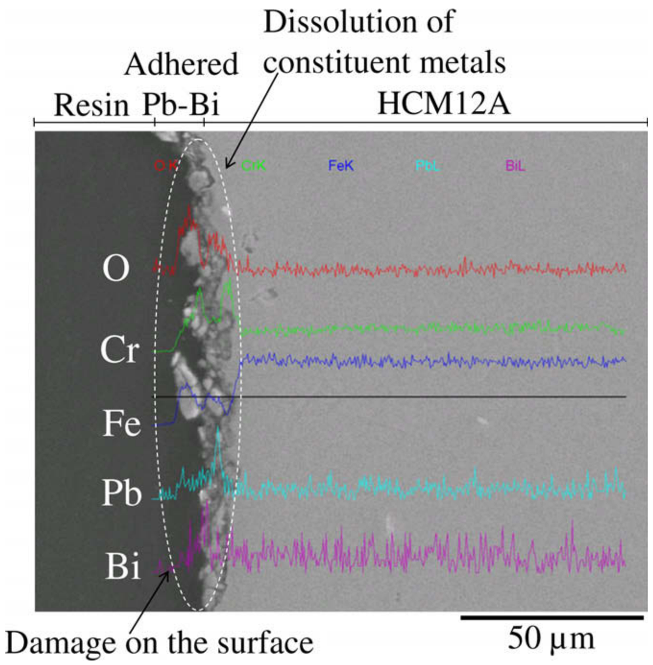

**Fig. 4.** SEM-EDX micrograph analysis of HCM12A without coating after immersion in Pb–Bi under transient temperature case-1.

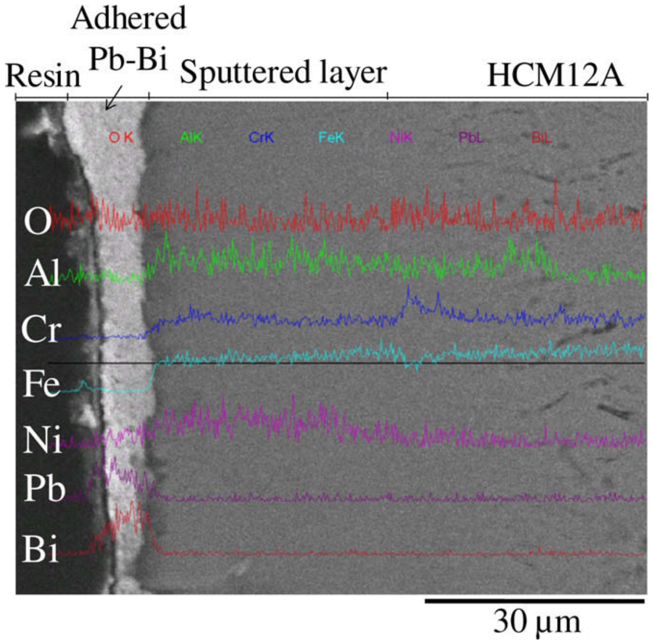

**Fig. 5.** SEM-EDX micrograph analysis of Al-SUS304-sputtering coated HCM12A after immersion in Pb–Bi under transient temperature case-1.

the $Ti_3SiC_2$ after immersion in Pb–Bi under transient temperature case-1. The figure shows that no penetration of Pb–Bi into the matrix of material and no dissolution of constituent metal from specimen into Pb–Bi occurred. The results showed that the SiC and $Ti_3SiC_2$ exhibited high corrosion resistance to Pb–Bi under transient temperature case-1.

### *3.2. Transient temperature condition case-2*

The aim of corrosion characteristics investigation of materials in Pb–Bi under the transient temperature condition case-2 is to predict corrosion resistance of materials if the transient temperature occurred in the reactor during steady operations of several hundred hours from start of operations. In this case, formation of oxide layer on the surface of steels is predicted. Therefore, the resistance of steels with protection of a protective oxide layer can be investigated. The results of testing under transient temperature condition case-2 are as follows.

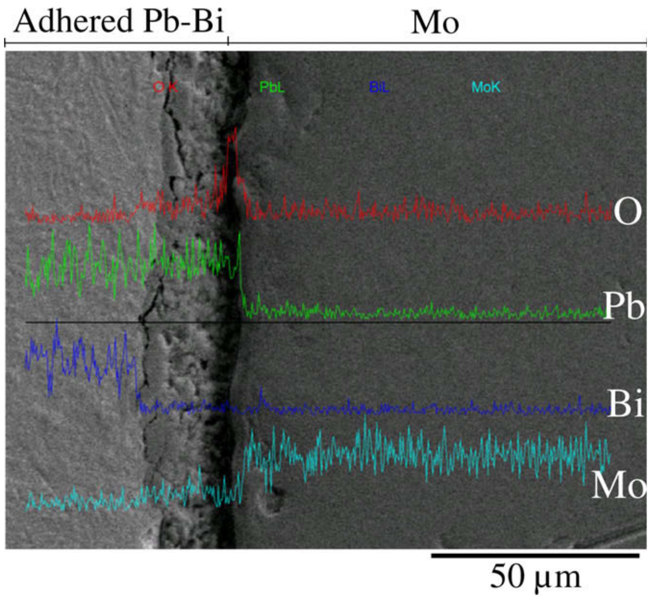

**Fig. 6.** SEM-EDX micrograph analysis of molybdenum after immersion in Pb–Bi under transient temperature case-1.

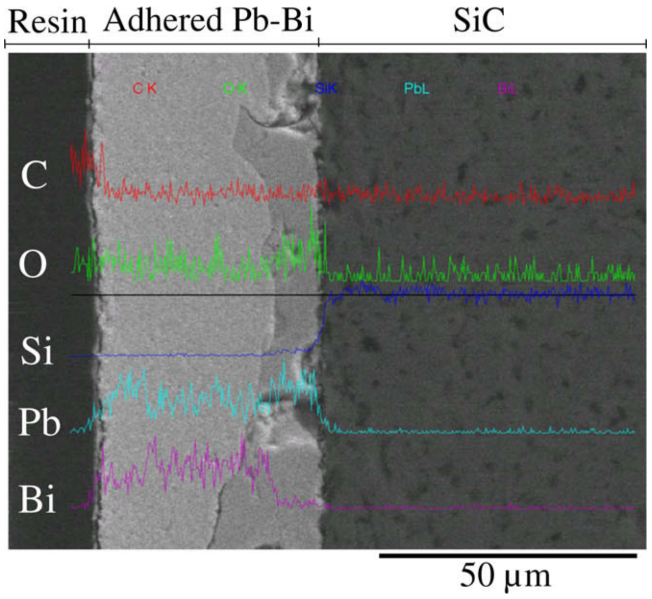

**Fig. 7.** SEM-EDX micrograph analysis of SiC after immersion in Pb–Bi under transient temperature case-1.

The results of high chromium steels after tested are shown in Figs. 9 and 10. Fig. 9 shows the SEM-EDX micrograph analysis of the cross section of Recloy10 after immersion in Pb–Bi under transient temperature case-2. As predicted, it is found that the multiple oxide layers were formed on the surface of Recloy10. However, mutual penetration of Pb–Bi into the oxide layers, and dissolution of constituent metals such as Si and Al from specimen into Pb–Bi of

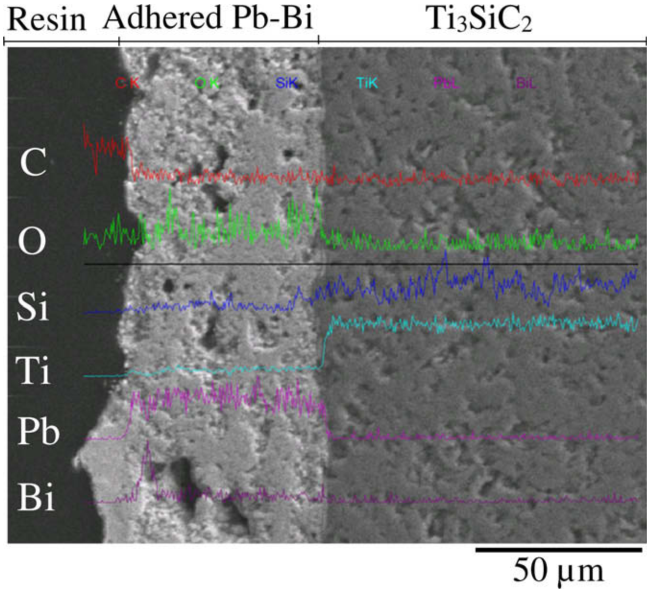

**Fig. 8.** SEM-EDX micrograph analysis of $Ti_3SiC_2$ after immersion in Pb–Bi under transient temperature case-1.

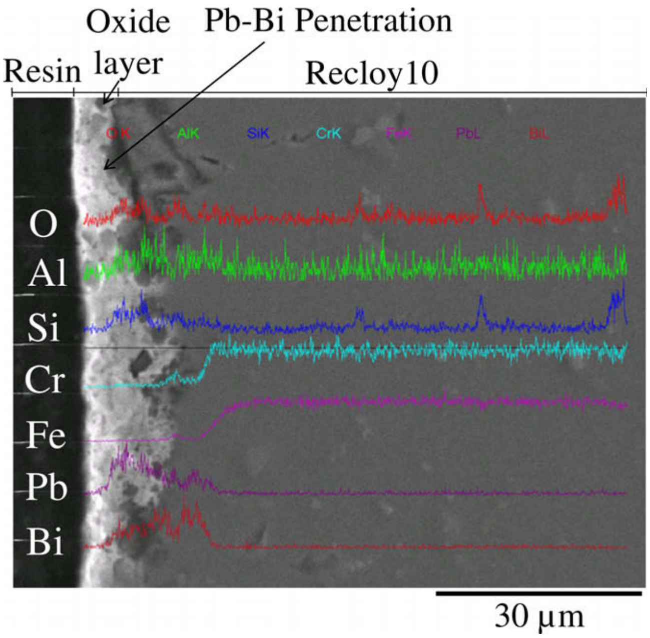

**Fig. 9.** SEM-EDX micrograph analysis of Recloy10 after immersion in Pb–Bi under transient temperature case-2.

6–13 µm in depth occurred. Fig. 10 shows the SEM-EDX micrograph analysis of the cross section of the SUS430 after immersion in Pb–Bi under transient temperature case-2. Similar to Recloy10, it is found that the multiple oxide layers were formed on the surface of SUS430. However, penetration of Pb–Bi into the oxide layers with 5–10 µm in depth occurred, accompanied by dissolution of constituent metals such as Fe, Cr as well as Si from the matrix into Pb–Bi.

The result of Al-SUS304-sputtering-coated SUS316 after tested is shown in Pb–Bi under transient temperature case-2 in Fig. 11. The figure shows that the coating layer remains intact on the base surface of the SUS316. There was no penetration of Pb–Bi into the matrix of material and no dissolution of constituent metals from material to Pb–Bi observed.

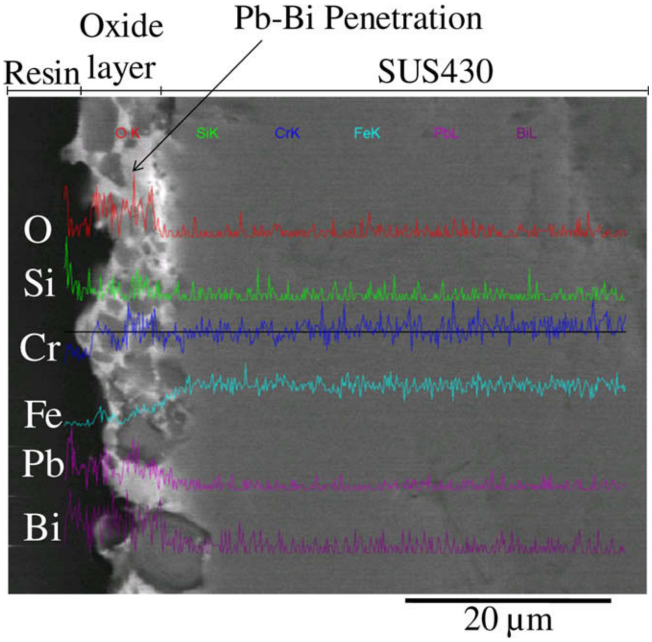

**Fig. 10.** SEM-EDX micrograph analysis of SUS430 after immersion in Pb–Bi under transient temperature case-2.

Fig. 12 shows the SEM-EDX micrograph analysis of the cross section of the molybdenum after immersion in Pb–Bi under transient temperature case-2. The figure shows that there was no penetration of Pb–Bi into the matrix of material and no dissolution of constituent metal from specimen into Pb–Bi.

Figs. 13 and 14 show the SEM-EDX micrograph analysis of the cross section of the ceramics after immersion in Pb–Bi under transient temperature case-2. Fig. 13 shows that there was no penetration of Pb–Bi into the matrix of SiC and no dissolution of the

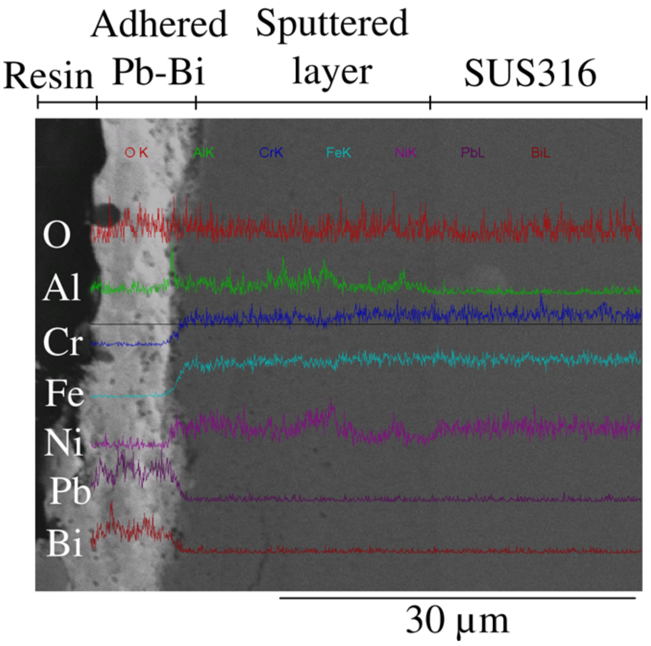

**Fig. 11.** SEM-EDX micrograph analysis of Al-SUS304-sputtering coated SUS316 after immersion in Pb–Bi under transient temperature case-2.

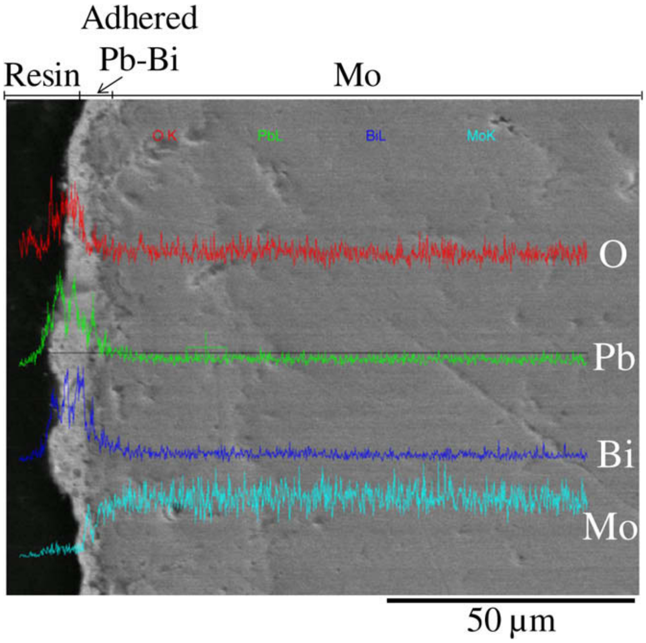

**Fig. 12.** SEM-EDX micrograph analysis of molybdenum after immersion in Pb–Bi under transient temperature case-2.

constituent metal from SiC into Pb–Bi. Fig. 14 shows that there was no penetration of Pb–Bi into the matrix of $Ti_3SiC_2$ and no dissolution of constituent metal from $Ti_3SiC_2$ into Pb–Bi. The results showed that the ceramics of SiC and $Ti_3SiC_2$ exhibited high corrosion resistance to Pb–Bi under transient temperature case-2.

## 4. Discussion

At least two phenomena occur for the materials because of transient temperature conditions in Pb–Bi from lower temperature to higher temperature, i.e. increasing solubility of metal elements into Pb–Bi and thermal expansion of the materials. Gromov reported that the solubility of metals in Pb–Bi will increases as temperature increases [1]. Thermal expansion of the materials will possibly allow the penetration of Pb–Bi into the grain boundaries. Moreover, the mechanical stress between oxide layer and substrate will also possibly occur because of different thermal expansion coefficients between oxide layer and substrate. It means that resistance of materials to corrosion attack from Pb–Bi under transient temperature conditions from lower temperature to higher temperature will decrease, chemically and mechanically.

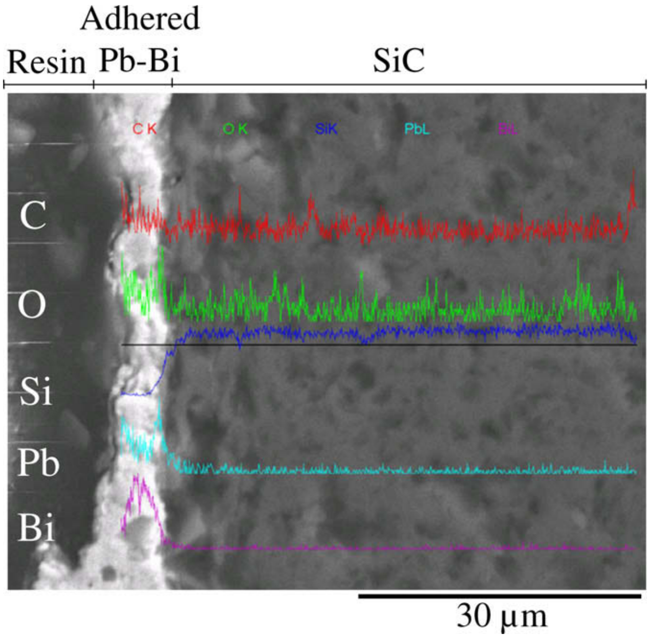

**Fig. 13.** SEM-EDX micrograph analysis of SiC after immersion in Pb–Bi under transient temperature case-2.

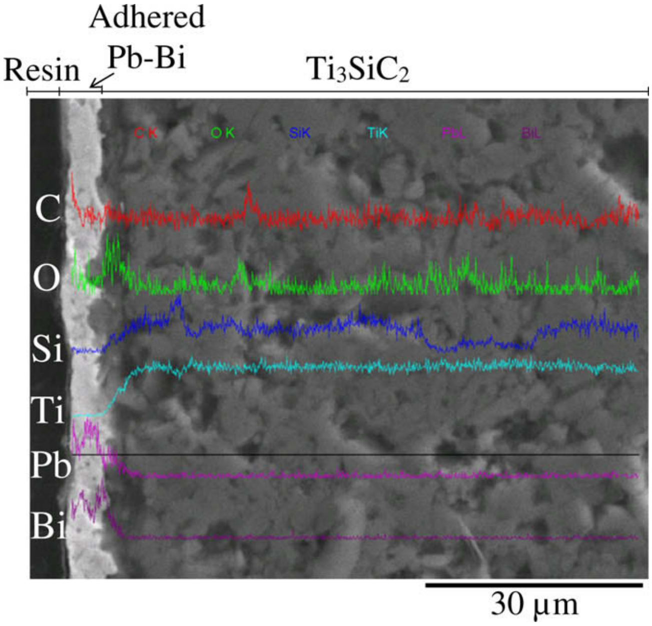

**Fig. 14.** SEM-EDX micrograph analysis of $Ti_3SiC_2$ after immersion in Pb–Bi under transient temperature case-2.

HCM12A, Recloy10 and SUS430 were reported exhibit corrosion resistance in Pb–Bi at steady temperature of 550 °C [6,7]. However, our results showed that corrosion trace of the materials in Pb–Bi under transient temperature of 550–800 °C occurred. For transient temperature case-1, the damage of the surface matrix of HCM12A was observed with the trace of Pb–Bi penetration. The surface condition indicated thermal expansion of the material, followed by corrosion attack by Pb–Bi and made the surface damage of HCM12A. For transient temperature case-2, penetration of Pb–Bi into the oxide layer of Recloy10 and SUS430 was found. The oxide layer was formed during 500 h immersion in Pb–Bi at 550 °C. Formation of the oxide layer on the surface of the materials after exposure to Pb–Bi at 550 °C was also reported by other researchers [6,7]. Nevertheless, in the transient temperature condition of Pb–Bi from lower temperatures to high temperatures up to 800 °C high dissolution rate of constituent metals of the specimens and thermal expansion of the oxide layer structure cause the corrosion attack mechanism of Pb–Bi. However, splitting of the oxide layer because of mechanical stress due to different thermal expansion coefficients between the oxide layer and the substrate was not found.

Opposite to the high chromium steels, there was no penetration of Pb–Bi and no dissolution of constituent metals from matrix of specimens into Pb–Bi for Al-SUS304-sputtering coated steels for all transient temperature conditions cases. The phenomena exhibit that sputtering layer produced by UBMS technique has good corrosion resistance to corrosion attack of Pb–Bi even under transient temperature conditions of 550 °C to 800 °C.

Refractory metal of molybdenum and ceramics of SiC and $Ti_3SiC_2$ show good corrosion resistance in Pb–Bi under transient temperature of 550 °C to 800 °C in this investigation. Dissolution of constituent metals into Pb–Bi did not occur. Protection from corrosion attack of Pb–Bi was derived from low solubility of the materials in Pb–Bi even at elevated temperature. Nevertheless, thermal expansion of the materials at high temperature which will promote penetration of Pb–Bi along the grain boundaries have to be considered. However, there was no penetration of Pb–Bi into the matrix of the specimens for all transient temperature conditions cases in the present study.

## 5. Conclusions

The corrosion characteristics of Al-SUS304-sputtering-coated steels, high chromium steels, a refractory metal and ceramics have been investigated after immersion in Pb–Bi under transient temperature conditions of 550–800 °C. The fully dense Al-SUS304 coating layer which was produced by using UBMS technique could protect the steels from corrosion attack of Pb–Bi. On the other hand, high chromium steels of HCM12A, Recloy10 and SUS430 could not withstand corrosion attack by Pb–Bi. A refractory metal of molybdenum exhibits high corrosion resistance to Pb–Bi. Ceramics of SiC and $Ti_3SiC_2$ also exhibit high corrosion resistance to Pb–Bi under transient temperature conditions.

## Acknowledgement

The authors would like to express their gratitude to Mr. T. El-Raghy, Ph.D. of 3-ONE-2 LLC for his supply of $Ti_3SiC_2$.

## References

[1] B.F. Gromov, Y.I. Orlov, P.N. Martynov, V.A. Gulevsky, in: Proceedings of Heavy Liquid Metal Coolant (HLMC) 1999, p. 87.
[2] M. Takahashi, H. Sekimoto, K. Ishikawa, T. Suzuki, K. Hata, S. Que, S. Yoshida, T. Yano, M. Imai, in: Proceedings of the 10th International Conference on Nuclear Engineering (ICONE10), 14–18 April 2002, Arlington, Virginia, USA, ICONE10-22226.
[3] E.P. Loewen, A.T. Tokuhiro, J. Nucl. Sci. Technol. 40 (8) (2003) 614.
[4] A.K. Rivai, M. Takahashi, Prog. Nucl. Energy 50 (2008) 560.
[5] G. Müeller, A. Heinzel, J. Konys, G. Schumacher, et al., J. Nucl. Mater. 301 (2002) 40.
[6] M. Kondo, M. Takahashi, J. Nucl. Mater. 356 (2006) 203.
[7] M. Kondo, M. Takahashi, N. Sawada, K. Hata, J. Nucl. Sci. Technol. 43 (2) (2006) 107.
[8] G. Müller, G. Schumacher, F. Zimmermann, J. Nucl. Mater. 278 (2000) 85.
[9] Y. Kurata, M. Futakawa, S. Saito, J. Nucl. Mater. 335 (2004) 501.
[10] A. Heinzel, M. Kondo, M. Takahashi, J. Nucl. Mater. 350 (2006) 264.
[11] C. Fazio, I. Ricapito, G. Scaddozo, G. Benamati, J. Nucl. Mater. 318 (2005) 325.
[12] M. Takahashi, M. Kondo, in: Proceedings of the GLOBAL 2005, 9–13 October 2005, Tsukuba, Japan, Global 2005-425.
[13] K. Hata, M. Takahashi, in: Proceedings of the GLOBAL 2005, 9–13 October 2005, Tsukuba, Japan, Global 2005-446.
[14] L. Martinelli, F. Balbaud-Célérier, A. Terlain, et al., Corros. Sci. 50 (2008) 2523.
[15] O. Yeliseyeva, V. Tsisar, G. Benamati, Corros. Sci. 50 (2008) 1672.
[16] S. Zaki, H. Sekimoto, Nucl. Eng. Des. 162 (1996) 205.
[17] M. Takahashi, S. Uchida, Y. Yamada, K. Koyama, Prog. Nucl. Energy 50 (2008) 269.
[18] A. Romano, P. Hezlar, N.E. Todreas, Nucl. Technol. 147 (3) (2004) 368.
[19] A. Weisenburger, K. Aoto, G. Müller, A. Heinzel, G. Schumacher, T. Furukawa, J. Nucl. Mater. 358 (2006) 69.
[20] A. Doubková, F. DiGabriele, P. Brabec, E. Keilová, J. Nucl. Mater. 376 (2008) 260.
[21] M.W. Barsoum, L.H. Ho-Duc, M. Radovic, T. El-Raghy, J. Electrochem. Soc. 150 (4) (2003) B166.
[22] M.W. Barsoum, T. El-Raghy, J. Am. Ceram. Soc. 79 (7) (1996) 1953.
[23] R.I. Bates, R.D. Arnell, Surf. Coat. Technol. 89 (1997) 204.
[24] B. Window, N. Savvides, J. Vac. Sci. Technol. A 4 (2) (1986) 196.
[25] B. Window, N. Savvides, J. Vac. Sci. Technol. A 4 (3) (1986) 453.
[26] N. Savvides, B. Window, J. Vac. Sci. Technol. A 4 (3) (1986) 504.